Original Paper

Partial Decellularization as a Method to Improve the Biocompatibility of Heart Tissue Implants

Mihai Meşină[1], Ion Mîndrilă[2], Mihaela Iustina Meşină-Botoran[2], Laura Andreea Mîndrilă[1], Ionica Pirici[2]

[1]*Doctoral School, University of Medicine and Pharmacy of Craiova*

[2]*Department of Anatomy, Faculty of Medicine, University of Medicine and Pharmacy of Craiova*

ABSTRACT: Increasing the biocompatibility of some biological implants through tissue engineering is important for regenerative medicine, which recently has a rapid development dynamic. In this study we used tree different washing protocols, respectively with Sodium Lauryl Sulfate (SLS), with Sodium Deoxycholate (SD), and with saline (Sa) to achieve partial decellularization of 2-3mm thick cross-sections through Wistar rat hearts. Pieces of the heart tissue were either histologically analyzed to evaluate the decellularization processes or implanted for 5 days on 9-day-old chick embryo chorioallantoic membrane (CAM) and then histologically analyzed to evaluate CAM-implant interactions. Histological analysis of SLS or SD washed tissues showed different microscopic features of the decellularization processes, SLS-washing leading to the formation of a completely decellularized ECM layer at the periphery of the heart tissue. Both detergents induced changes in the spatial arrangement of collagen fibers of the heart tissue. Histological analysis of the CAM implants shoved that the peripheral zone with complete decellularization induced by SLS increased the biocompatibility of heart tissue implants by favoring neovascularization and cell migration. These results suggested that the biocompatibility of the heart tissue implant can be modulated by the appropriate use of a SLS-based decellularization protocol.

KEYWORDS: Extracellular matrix, decellularization, heart tissue, sodium lauryl sulfate, sodium deoxycholate, chorioallantoic membrane.

Introduction

Increasing the biocompatibility of biological implants through tissue engineering is important for regenerative medicine, which has recently had a rapid development dynamic, since the reconstruction of some tissues and organs by repopulating decellularized ECM scaffolds with stem cells was successful [1].

Tissues and organs decellularization were used for ECM isolation by cellular lysis, solubilization and cellular components removal; to achieve these goals, a wide variety of chemical, physical, enzymatic or a combination of those methods were used [1,2].

The most widely used methods includes sequences of hypo and hyperosmolar shocks to induce cell lysis, enzymatic proteolysis, and dissolution and removal of cellular material using either an ionic detergent such as SLS [3-5] and SD [6], or non-ionic deter-gent like Triton X-100 [7].

The decellularization process is obtained by use of chemical baths, by fall pressure or pulsatile centrifugal pump perfusion [8-10], or by direct tissue-penetration capability of the supercritical fluids, using carbon dioxide at a pressure of 15 MPa and a temperature of 37°C [11].

Various organs have been successfully decellularized to obtain biologic scaffolds with potential in tissue engineering [12].

The first organs decellularized were the ones with a less complex architecture such as skin for the treatment of burn victims [13], cornea used in reconstructive surgery [14], heart valves with applications in the surgical treatment of valvular disease [15] or the urinary bladder [16] with many uses including tympanic surgery [17], esophageal reconstruction [18], tracheal plasty [19], or larynx surgery [20].

As the process was perfected, it expanded into liver decellularization [21,22], whole heart [23,24], kidney [25] or pancreas [26] decellularization.

The first decellularized heart scaffold was obtained in 2008 [23] using a perfusion-based method, and since then cardiac tissue has remained one of the most intensively studied organs subjected to the decellularization process [27].

A common approach was the use of detergent-based protocols, and of these the most studied were SLS, SD, and Triton X-100 [28].

SLS breaks non-covalent bonds, solubilizes cell membranes and is effective in removing nuclear materials [29], but alters the microstructure and biomechanical integrity of the ECM, affecting the ECM matrisome by removing fibronectin, glycosamino-glycans and proteoglycans [29-31].

Residual SDS from the decellularized matrix is difficult to remove, and through its cytotoxic effect can affect recellularization [27].

SD solubilizes cell membranes but is less effective in removing nuclear materials [32].

At the same time, it alters less the proteoglycan and collagen content of the ECM, which can favor recellularization [32,33].

The CAM begins to form from day 3 of the chick embryo development following a process of adhesion between the allantoic mesoderm and the chorionic mesoderm.

As a result, the CAM will have a chorionic epithelial layer, a mesodermal layer and an allantoic epithelial layer in its structure [34,35].

Due to the rich vascular network of the meso-dermal layer [35], CAM has proven to be a powerful and widely used tool in the study of angiogenesis, tumor growth and migration, or for evaluation of the biological properties of some nanocomposites [36-38].

CAM has been used in tissue engineering for several decades, being used not only for testing the angiogenic potential of the constructed material but also for testing its biocompatibility [39-42].

Tissues-engineered materials can be used to replace damaged or missing tissues.

In vivo, the lack of rapid revascularization can lead to the destruction of the implanted material [40].

The biochemical and structural information preserved by the natural ECM can activate the cellular functions involved in tissue regeneration, which makes decellularized ECM one of the most used biomaterials in the clinic [43].

Decellularized ECM can lead to increased vascularization of the implants, can act as an optimal environment for cells sustenance, proliferation, and distribution and can be used to increase the bioavailability of tissues in regenerative medicine [44].

Therefore, the generation of a decellularized ECM layer on the surface of an implant can be considered when improving its biological properties is the desired goal.

Starting from these observations, we considered that the presence of a decellularized ECM layer at the periphery of an implant can improve its integration in the host tissue and therefore increase its biocompatibility.

In this study we used some decellularization protocols based on a single detergent, namely SD and SLS, to partially decellularize fragments of rat heart tissue.

These fragments were implanted on 9-day-old CAM for 5 days, and then were analyzed histologically to evaluate the processes of their revascularization and repopulation with cells from the mesoderm layer of the CAM.

Materials and Methods

Animals
The experimental protocol on animals was first approved by the Committee of Ethics and Scientific Deontology of the University of Medicine and Pharmacy of Craiova (139/20.12.2019).

Hearts harvested from 9 ten-week-old male Wistar rats were used for the decellularization procedures.

Under general anesthesia with Ketamine (100mg/Kg) and Xylazine (10mg/Kg) a median thoraco-abdominal incision was made to access the superior and inferior vena cava and thoracic aorta.

After dissection of the great vessels at the base of the heart, the arteries of the aortic arch (brachiocephalic trunk, left common carotid and left subclavian arteries) and the superior vena cava were ligated and sectioned, and the inferior vena cava, in the suprahepatic portion, and the thoracic aorta, in thoracic portion, were cannulated with an 18G needle.

Normal saline serum was infused on the cannula inserted in the inferior vena cava for 30 minutes, to obtain exsanguination of the cardio-pulmonary complex.

The cardio-pulmonary complex was harvested, washed abundantly with saline, and then the aorta was infused for 60 minutes with saline at a hydro-static pressure of 100cm H2O.

Next, 2-3mm thick cross-sections through ventricles were made and placed in plastic tissue embedding cassettes, which were attached to a gentle vertical shaking system.

Decellularization protocols
The washing protocols with SLS, SD or Sa were applied in parallel, with identical development times.

Hypoosmotic shock was initially produced by washing for 60 minutes the sections with distilled water and then with phosphate-buffered saline solution (PBS) for another 60 minutes.

Next, the heart cross-sections were placed for 18 hours in Sa (n=3), 2% SLS (n=3), respectively 2% SD (n=3).

Finally, the heart cross-sections were washed with PBS for 120 minutes.

The processed heart cross-sections were sectioned symmetrically.

One-half of the cross-section was fixed (48h) in 10% neutral buffered formalin and used for histological analysis.

The other half was cut into 2-3mm pieces (n=5) that were implanted on the 9-day-old CAM.

The CAM assays

White fertilized Leghorn eggs were used to obtain 9-day-old CAM.

They were incubated at 37.5°C and 70% humidity, being rotated 2 times/day.

After 3 days the eggs were examined with an ovoscope to identify and mark on the shell the site of embryo development and the air chamber.

The shell was sterilized with a swab soaked in 70% alcohol.

Using an 18G syringe, 3.5-4ml of albumen were extracted from the pole opposite the air chamber.

The site of embryo was covered with 1.5cm square patch of scotch tape and a round window with a diameter of 1cm was made with a scissors.

After checking the viability of the embryos, the windows were covered with tape and the eggs were re-incubated until day 9, when the CAM is sufficiently developed to allow the implantation of heart tissue xenografts.

The 2-3mm pieces of processed heart tissue (n=3 for each heart cross-section) were implanted, by applying to the surface of the CAM, after gentle abrasion of the implantation site beforehand.

On the 14th day of development, the implanted fragments were harvested with the surrounding CAM and fixed (48h) in 10% neutral buffered formalin for histological analysis.

Histological analyses

Formalin fixed heart tissues and harvested CAM implants were processed using standard histological methods for paraffin embedding, sectioning at 7µm thickness, staining with H&E and Azan trichrome, and examined under light microscopy for morphological and morphometric evaluation.

The relative area of the CAM vessels in the implant area was determined by reporting the values obtained by measuring the area of visible vessels on the lower side of the CAM in the implant area and the area occupied by the implant on the CAM, using the Image-Pro Plus image processing and analysis software.

Statistical Analysis

The results are presented as mean±standard deviation, and data were compared using a one-way ANOVA with Tukey's post hoc analysis having set the significance level at 0.05.

For data analysis SPSS version 16 (SPSS, Inc., Chicago, IL, USA) was used.

Results

Histological analyses of the decellularization heart cross-sections

The macroscopic examination of the cardio-pulmonary complexes revealed a good removal of blood from the myocardial tissue, after retrograde perfusion of the heart for one hour with saline solution at a pressure of 100cm H_2O (Figure 1a,b).

The analysis of the cross-sectional surfaces through the ventricles before and after performing the washing protocol with SD (Figure 1c), SLS (Figure 1d) or Sa (Figure 1e) showed a reduction of their areas by 47.34±1.08%, 54.71±2.02%, respectively 2.16±0.21% (Figure 2k).

H&E and trichrome Azan staining did not identify any remaining nuclear material in the heart cross-sections, after washing for 18 hours with 2% SD (Figure 2a-d) or SLS (Figure 2e-h).

Histology of the SD-washed heart cross-sections

A first aspect highlighted by the light microscope analysis was the presence of thick corkscrew-like collagen bands visible on the entire surface of the cross-section through the heart (Figure 2a-c).

SD washing has been associated, in addition to the absence of basophilic material in the H&E staining (Figure 2d), with muscle cell lysis that was more advanced in the peripheral area of the heart tissue.

In this area, the muscle fibers are no longer identifiable, and the corkscrew-shaped collagen bands had an irregular orientation (Figure 2b).

The central area of the heart tissue piece showed less obvious cell lysis, and at its level the identification of muscle fiber bundles was still possible.

In this area, the corkscrew-like collagen bands had a regular arrangement, being parallel to the bundles of muscle fibers (Figure 2c).
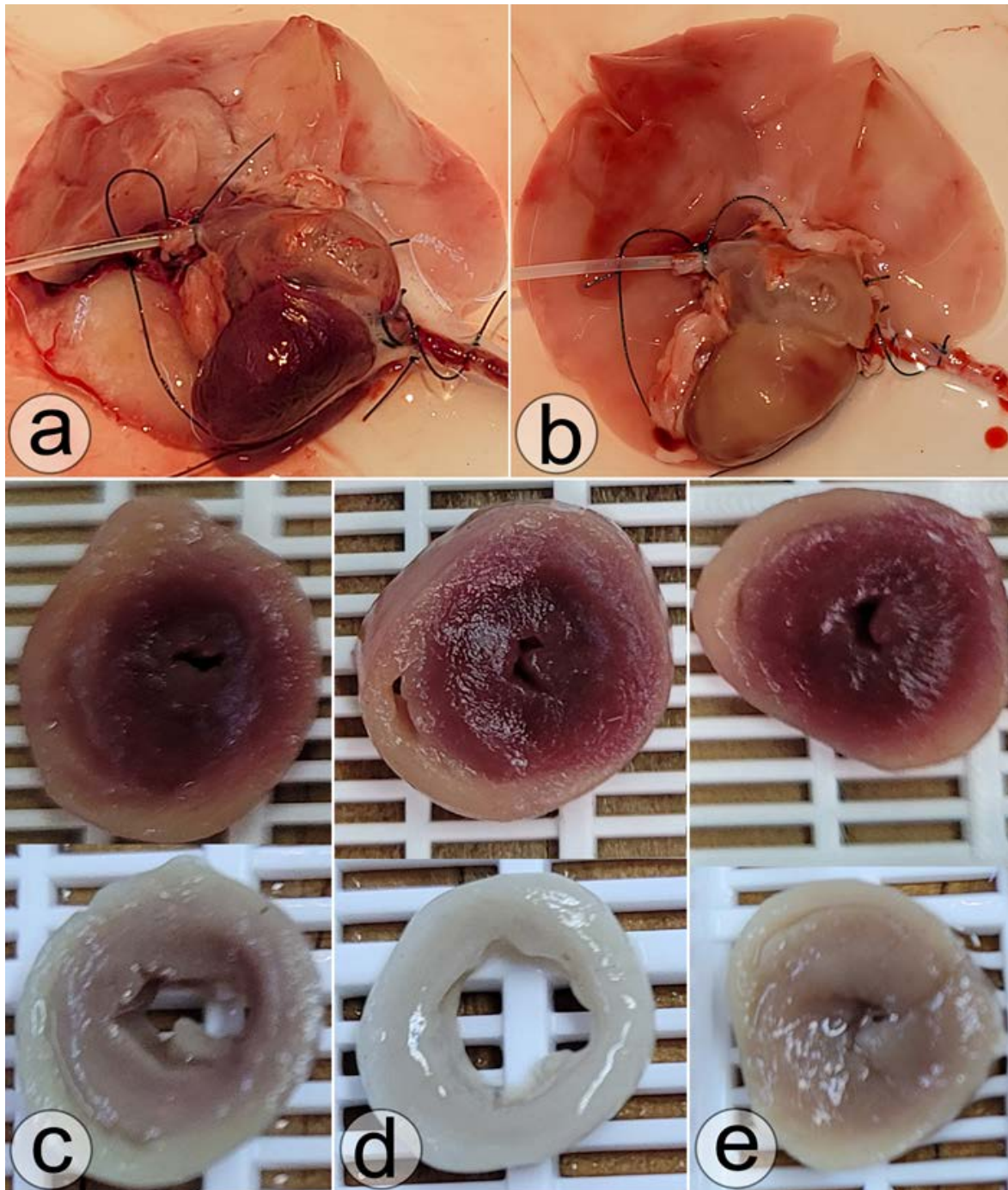
Figure 1. The cardio-pulmonary complexes before (a) and after (b) retrograde Sa per-fusion for 60 minutes at a pressure of 100cm H2O. Macroscopic features of the ventricular cross-sections before and after the washing protocols with SD (c), SLS (d) or Sa (e) were applied.

Histology of the SLS-washed heart cross-sections

The histological analysis of the SLS-washed heart tissue pieces highlighted a peripheral area with completely decellularized ECM in which all the cell lysis material was removed, and the collagen fibers formed an irregular three-dimensional network in which the corkscrew-shaped collagen fibers were no longer clearly identified (Figure 2e,f).

This is separated by a narrow band of advanced cell lysis from the central zone, where the bundles of muscle fibers could be individualized, and among them the corkscrew-shaped collagen bands could still be identified (Figure 2g).
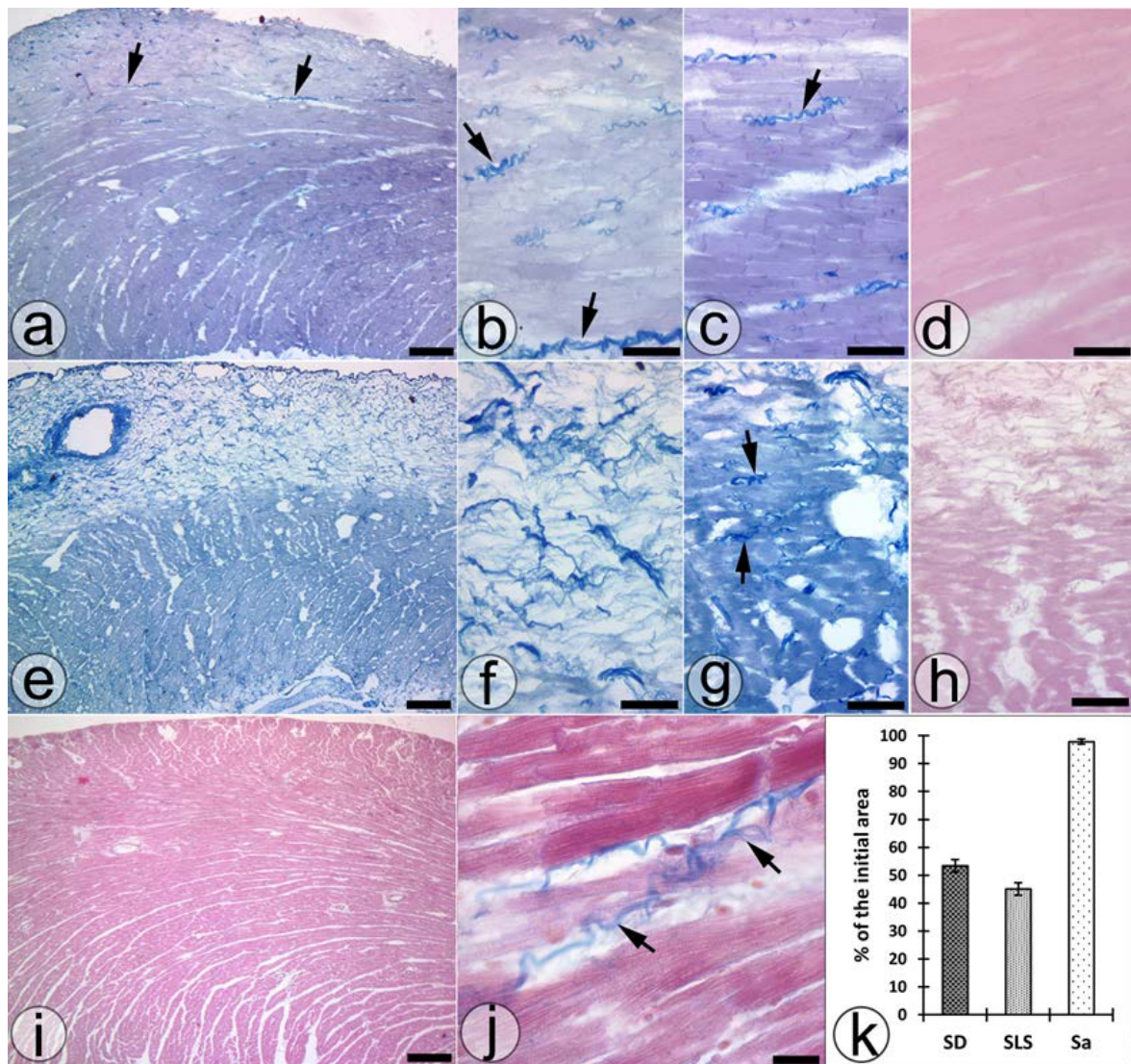
Figure 2. Histologically appearance of the heart cross-sections after the washing protocols with SD (a-d), SLS (e-h) or Sa (i,j) were applied. Variations of the heart cross-section surface areas induced by washing protocols (k). Black arrows point to corkscrew-shaped collagen bands. Bare=500µm (a,e,i); 50µm (b-d,f-h), and 20µm (j). Azan trichromic (a-c,e-g,i,j) and H&E (d,h) staining.

Histology of the Sa-washed heart cross-sections

In these heart tissue pieces, rare areas with incipient cell lysis were identified in which thick bands of collagen that outlined corkscrew shapes could be highlighted between the bundles of muscle fibers.

The nuclear component was not influenced by this washing protocol (Figure 2i,j).

CAM assay

The implantation of the heart decellularized pieces (Figure 3a) on the 9-day-old CAM (Figure 4b) was followed by the specific pattern development of the underlying CAM vessels.

The measurement of the underlying CAM vessels areas showed a statistical difference between the three types of implants (Figure 3c), the vessels having a relative area of 35.81±2.17 in the case of the implants washed with Sa, 22.48±3.08 for those washed with SD, and 18.66±1.89 for those washed with SLS ($p < 0.05$, ANOVA with post-hoc Tukey test).

Vessels with spoke-wheel pattern were identified in the CAM thickness around the Sa or SD washed implants (Figure 3d,f).
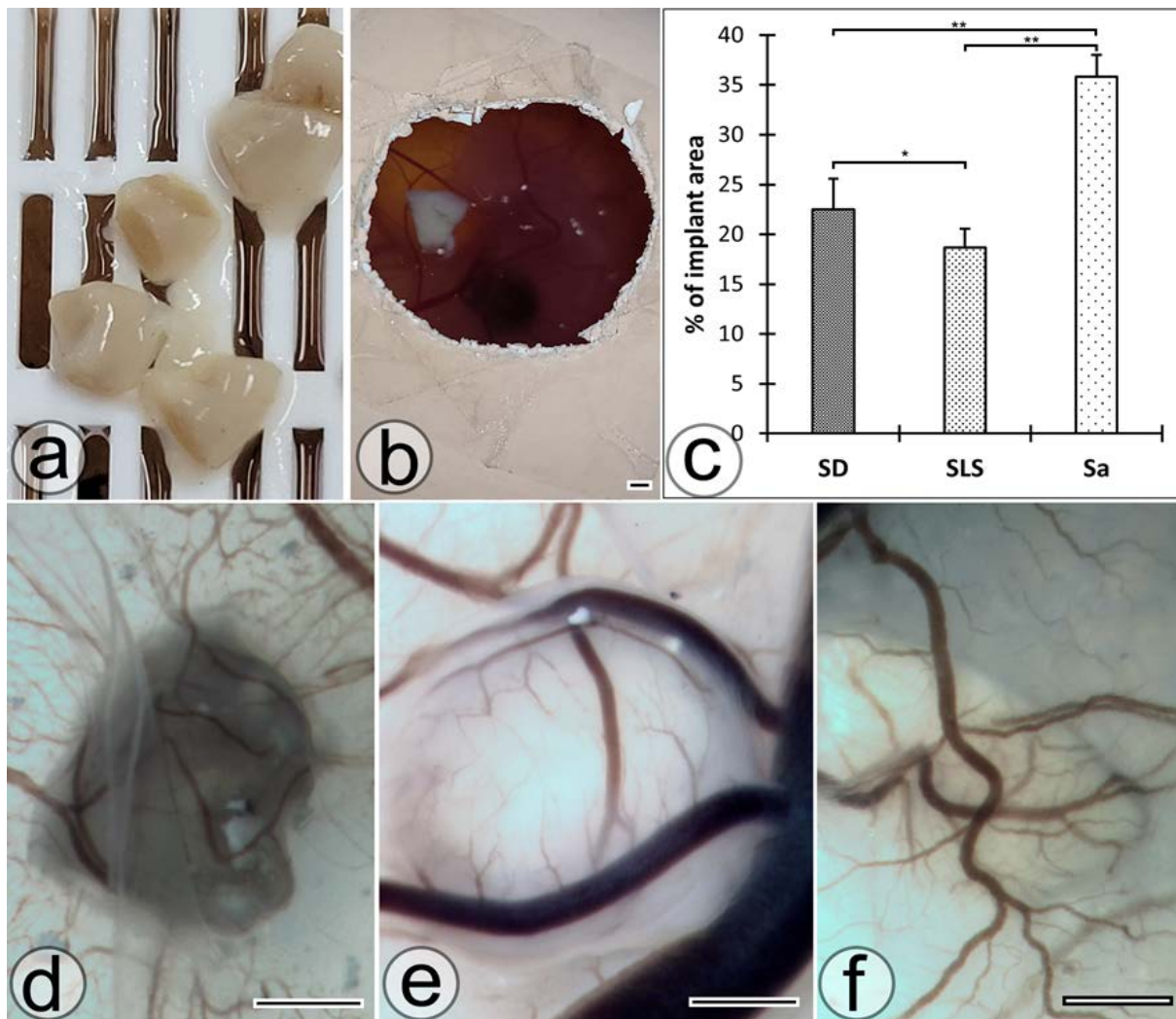
Figure 3. *Partially decellularized heart tissue fragments (a) implanted on the 9-day-old CAM (b). Variations of the relative area of the vessels of the CAM which supports the bottom face of the implant (c) (*p<0.05; **p<0.01). The macroscopic features of the CAM vessels in the implant areas 5 days after the application of heart tissue fragments washed with S (d), SLS (e) or Sa (f) (bottom faces of the harvested and formalin fixed CAM-implant complexes). Bar=1mm.*

Histological analyses of the Sa-washed heart tissue implants

The histological analysis highlighted a rich inflammatory infiltrate with numerous heterophiles in the heart tissue implant area adjacent to the CAM-implant interface.

These heterophiles entered the thickness of the heart tissue implant among the bundles of muscle fibers and blocked the CAM mesenchymal cells migration into the implant (Figure 4a,b).

The microscopic examination also showed a thick CAM and the presence of numerous vessels near the CAM-implant interface (Figure 4b).

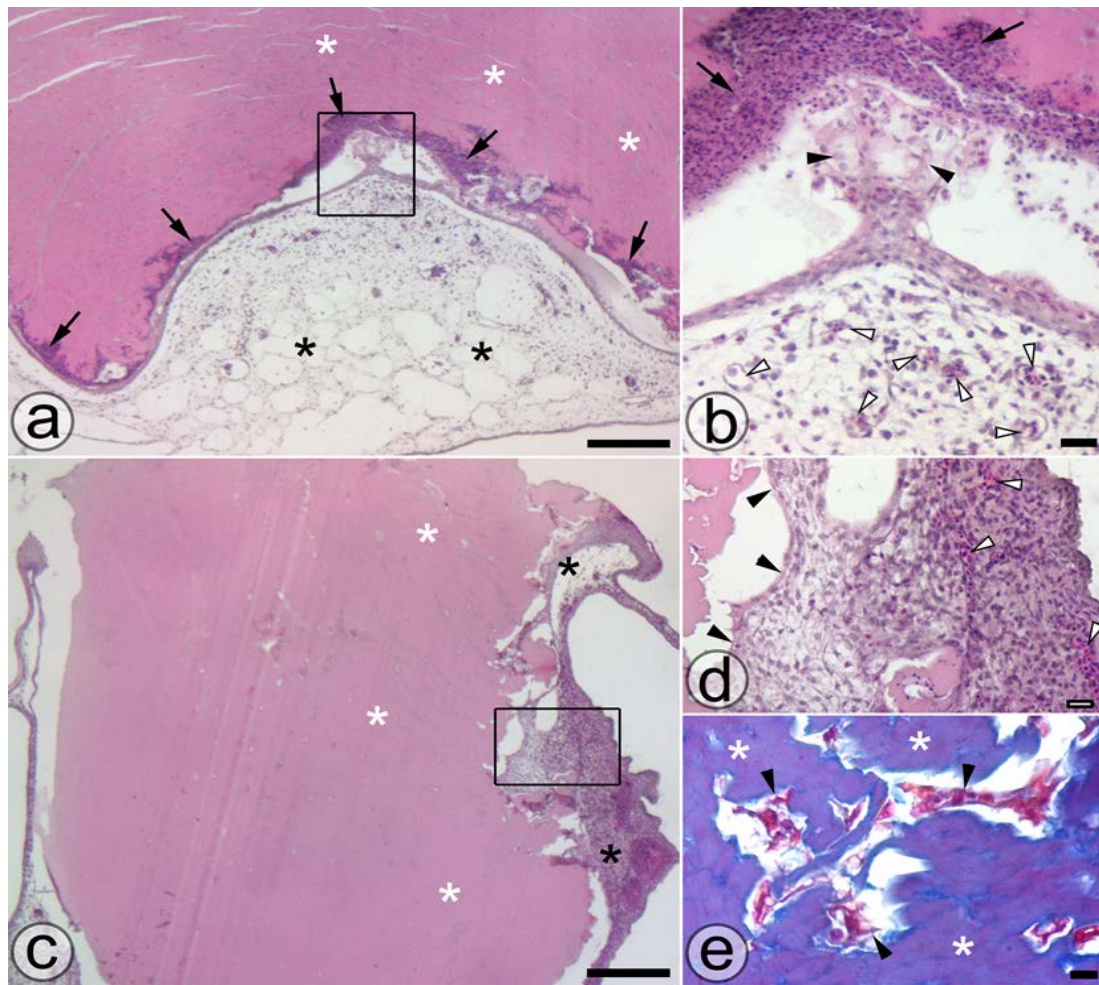No CAM vessels were identified to enter the heart tissue implant.

Figure 4. Histological features of the Sa-washed (a, b) and SD-washed (c-e) heart tis-sue implants (white stars) 5 days after implantation on CAM (black stars). Inflammatory infiltrates were marked with black arrows, cells migrated from the mesenchymal layer of the CAM with black arrowheads, and CAM vessels with white arrowheads. Bare=500μm (a,c), 20μm (b,d) and 10μm (e). H&E (a-d) and Azan trichromic (e) staining.

Histological analyses of the SD-washed heart tissue implants

The histological analysis highlighted clusters of mesenchymal cells that invaded the heart tissue implant near the CAM-implant interface (Figure 4c,d), some migrating for short distances among the bundles of partially decellularized muscle fibers (Figure 4e).

The invasion of the mesenchymal cells of the CAM occurred only at the periphery of the heart tissue implant, in the areas with advanced decellularization.

No inflammatory infiltrate was identified around the CAM-implant interface.

The CAM under the implant showed an increased density of the mesenchymal cellular component (Figure 4d).

Histological analyses of the SLS-washed heart tissue implants

The histological analysis showed the integration of the completely decellularized peripheral area of the SLS-washed heart tissue implant into the CAM thickness. (Figure 5a,b).

This area repopulated by CAM mesenchymal cells was characterized by the presence of numerous neo vessels and the absence of inflammatory infiltrate near the CAM-implant interface (Figure 5c).

Neo vessels and mesenchymal cells, some with the fibroblastic-like appearance, were observed among the bands of partially decellularized muscle fibers of the implant.

The border between the completely decellularized peripheral area and the partially decellularized central area of the implant was marked in some places by the presence of an inflammatory infiltrate (Figure 5b,f).
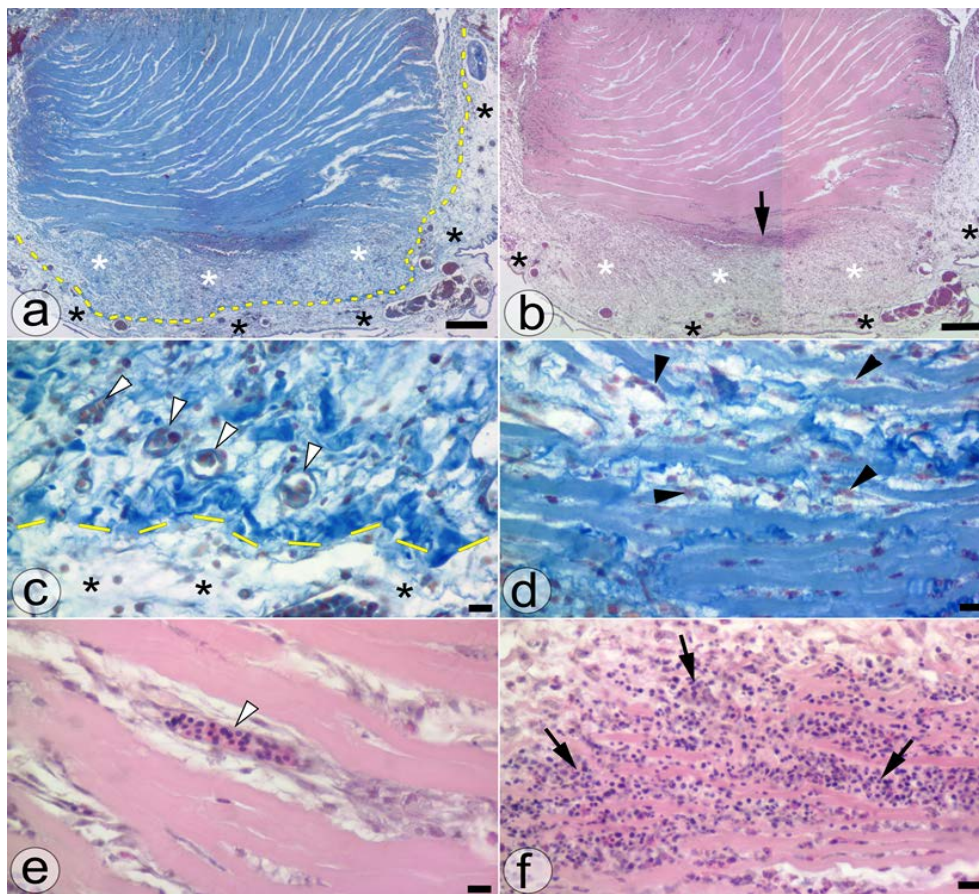
Figure 5. Histological features of the SLS-washed heart tissue implant 5 days after implantation on CAM (black stars). Inflammatory infiltrates with numerous heterophiles were marked with black arrows, mesenchymal cells of CAM with black arrowheads, and CAM vessels with white arrowheads. Bare=500μm (a,b), 20μm (c,d) and 10μm (e,f). H&E (b,e,f) and Azan trichromic (a,c,d) staining.

Discussion

Cardiac muscle has a complex structure optimized for lifelong pumping function which is difficult to replicate in vitro [45].

Collagen, fibronectin, and elastin are the main components of cardiac ECM, which ensure the durability, strength, and flexibility of the heart [46].

Recently, the development of single ionic detergent-based protocols for cardiac tissue decellularization has been especially studied because they are cheap, quick, and can produce the lysis of cell membranes with the removal of cellular components and nuclear materials [27,28,47].

At the same time, a series of undesirable effects of these detergents have been reported, represented by the alteration of the ECM matrisol and the persistence of the detergent in the ECM, with the impeding of the recellularization process [29,48].

These effects have been reported especially in the case of the use of SLS, which modifies the 3D conformation of the ECM by removing fibronectin, glycosaminoglycans, proteoglycans, ECM regulators, and by altering the collagen structure [30].

Our histological analysis showed that even in the case of incomplete decellularization of the heart cross-sections, both washing protocols for 18 hours with 2% SLS or 2% SD had the effect of altering the ECM spatial arrangement, manifested by changing the area of the heart cross-sections and the morphological features of the collagen fibers (with the formation of corkscrew-like bands of collagen) (Figure 1, Figure 3).

These ECM changes were more advanced in the case of SLS washed heart cross-sections, in which thick cork-screw-shaped collagen bands were fragmented and disappeared in the peripheral area, with complete decellularization of the ECM (Figure 2f).

Therefore, keeping the ECM's spatial disposition unchanged cannot be a viable option when using SLS or SD based decellularization protocols.

To keep the collagen structure of the ECM as intact as possible, multiple detergent-based protocols must be used [49].

On the other hand, short-term washing with 2% SLS proved to be an acceptable method when the goal is to generate a layer of completely decellularized ECM on the surface of an implant.

Although it altered the three-dimensional structure of collagen and produced muscle cell lysis, the washing protocol with 2% SD is not suitable for this purpose.

CAM has had multiple uses in tissue engineering research proving to be a suitable tool for the analysis of angiogenesis and neovascularization of ECM scaffolds due to the ability of mesenchymal vessels to form new plexuses in the vicinity of the chorionic layer between days eight and fourteen of ontogenesis [36].

Although the chick embryo is naturally in a stage of immunodeficiency until the 18th day of development, heterophils, which are analogues of mammalian neutrophils, and macrophages can be observed inside the chick circulation from the 4th day of development [38].

As a result, the CAM assay allows, in addition to evaluating the revascularization process, an evaluation of the inflammatory reaction induced by the partially decellularized heart tissue implant. In our study, heart tissue implants had different effects on the vessels of the underlying CAM (Figure 3d,e,f).

The surface of the vessels visible on the lower side of the CAM showed an inverse variation with the degree of decellularization of the implant, having lower values for the implants washed with SLS and higher values for those washed with Sa (Figure 2).

Although the vascularity of the underlying CAM was richer, no vessels were identified within the heart tissue implants subjected to the Sa or SD washing protocols.

On the other hand, numerous neovessels originating in the CAM vessels were observed crossing the CAM-implant interface to revascularize the completely decellularized ECM of the SLS washed heart tissue implant.

These vessels filled with chicken red blood cells formed a rich network among the collagen fibers of the ECM, from where they passed further to the central area of the implant through the spaces between the fascicles of incompletely decellularized muscle fibers (Figure 5c,e).

Any implanted material causes a chronic inflammatory immune response that persists until the implanted material is removed or degraded

and that constitutes a daunting challenge for the clinical use of biomaterials [50].

The angiogenic activity and inflammatory response of CAM are influenced by the chemical composition and architecture of the bioimplant [40], and our study showed that the heart tissue implant washed with Sa induced both angiogenesis and the inflammatory response of the CAM, which is a normal response of the CAM to a foreign body [51].

Interesting is the fact that the partially decellularized ECM layer at the periphery of the SD washed heart tissue implant seems to block the CAM inflammatory response and reduces the angiogenic action of the implant.

Lack of inflammatory reaction at the CAM-implant interface and its presence at the periphery of the partially decellularized area of the SDS-washed heart tissue implant can be attributed to the detergent, knowing that SDS residues are difficult to remove from the tissues and cause an inflammatory reaction [42].

Differences were also noted after analyzing the CAM mesenchymal cells migration in the three types of grafts.

Due to the abundance of the inflammatory infiltrate at the CAM-implant interface CAM mesenchymal cells invasion was absent in heart tissue implants subjected to the Sa washing protocol.

The implants subjected to the SD washing protocol had at the CAM-implant interface small superficial areas invaded by the CAM mesenchymal cells, which in turn presented a slight increase in cellularity in the area corresponding to the implant.

The completely decellularized ECM layer at the periphery of the implants subjected to the SLS washing protocol were completely invaded by the CAM mesenchymal cells.

Also, these cells were identified migrating among the bundles of partially decellularized muscle fibers in the central area of the implant.

It should be noted that these mesenchymal cells showed changes in shape, acquiring a fibroblastic appearance (Figure 5d).

These results showed that the peripheral layer of decellularized ECM allowed the integration of this area of the implant into the CAM structure and, moreover, favored the migration of vessels and mesenchymal cells of the CAM in the central, partially decellularized area of the implant.

The washing protocol with SLS proved to be superior to that based on SD when covering the implant with a layer of completely decellularized ECM is the desired goal.

Complementary studies are needed to optimize the concentration, washing time and removal of detergent traces from the implant.

The evaluation of the inflammatory reaction on the CAM assay is limited by the immaturity of the immune system of the chick embryo until the 18th day of ontogenesis [44], so additional studies on mammalian models must be performed to confirm the results highlighted by this study.

Conclusions

The results of this study showed that by engineering a peripheral layer of completely decellularized ECM, an improvement in the integration of the heart tissue implant into the CAM was obtained by stimulating neovascularization and cell migration and suggested the possibility of modulating the biocompatibility of implants by the appropriate use of a SLS-based decellularization protocols.

Conflict of interests

None to declare.

References

1. Choudhury D, Yee M, Sheng ZLJ, Amirul A, Naing MW. Decellularization Systems and Devices: State-Of-The-Art Review. Acta Biomater, 2020, 115:51-59.
2. Meşină M, Mîndrilă I, Mesina C, Obleagă CV, Istrătoaie O. A perfusion decellularization heart model-an inter-esting tool for cell-matrix interaction studies. J Mind Med Sci, 2019, 6(1):137-142.
3. Keshvari MA, Afshar A, Daneshi S, Khoradmehr A, Baghban M, Muhaddesi M, Behrouzi P, Miri MR, Azari H, Nabipour I, Shirazi R, Mahmudpour M, Tamadon A. Decellularization of kidney tissue: comparison of sodium lauryl ether sulfate and sodium dodecyl sulfate for allotransplantation in rat. Cell Tissue Res, 2021, 386(2):365-378.
4. Narciso M, Ulldemolins A, Júnior C, Otero J, Navajas D, Farré R, Gavara N, Almendros I. Novel Decellularization Method for Tissue Slices. Front Bioeng Biotechnol, 2022, 10:832178.
5. Jorba I, Uriarte JJ, Campillo N, Farré R, Navajas D. Probing Micromechanical Properties of the Extracellular Matrix of Soft Tissues by Atomic Force Microscopy. J Cell Physiol, 2017, 232(1):19-26.
6. Xiong G, Flynn TJ, Chen J, Trinkle C, Xu R. Development of Anex Vivobreast Cancer Lung Colonization Model Utilizing a Decellularized Lung Matrix. Integr. Biol, 2015, 7 (12):1518-1525.
7. Mendoza-Novelo B, Avila EE, Cauich-Rodríguez JV, Jorge-Herrero E, Rojo FJ, Guinea GV, Mata-Mata JL. Decellu-larization of pericardial tissue and its impact on tensile viscoelasticity and glycosaminoglycan content. Acta Biomater, 2011, 7(3):1241-1248.
8. Prasertsung I, Kanokpanont S, Bunaprasert T, Thanakit V, Damrongsakkul S. Development of acellular dermis from porcine skin using periodic pressurized technique. J Biomed Mater Res B Appl Biomater, 2008, 85(1):210-219.
9. Sano MB, Neal RE 2nd, Garcia PA, Gerber D, Robertson J, Davalos RV. Towards the creation of decellularized organ constructs using irreversible electroporation and active mechanical perfusion. Biomed Eng Online, 2010, 9:83.
10. Funamoto S, Nam K, Kimura T, Murakoshi A, Hashimoto Y, Niwaya K, Kitamura S, Fujisato T, Kishida A. The use of high-hydrostatic pressure treatment to decellularize blood vessels. Biomaterials, 2010, 31(13):3590-3595.
11. Sawada K, Terada D, Yamaoka T, Kitamura S, Fujisato T. Cell removal with supercritical carbon dioxide for acellular artificial tissue. J Chem Technol Biotechnol, 2008, 83(6):943-949.
12. Langer R, Vacanti J P. Tissue engineering. Science, 1993, 260(5110):920-926.
13. Feng X, Tan J, Pan Y, Wu Q, Ruan S, Shen R, Chen X, Du Y. Control of hypertrophic scar from inception by using xenogenic (porcine) acellular dermal matrix (ADM) to cover deep second degree burn. Burns, 2006, 32(3):293-298.
14. Shafiq MA, Gemeinhart RA, Yue BY, Djalilian AR. Decellularized human cornea for reconstructing the corneal epithe-lium and anterior stroma. Tissue Eng Part C Methods, 2012, 18(5):340-348.
15. Schmidt D, Stock UA, Hoerstrup SP. Tissue engineering of heart valves using decellularized xenogeneic or polymeric starter matrices. Philos Trans R Soc Lond B Biol Sci, 2007, 362(1484):1505-1512.
16. Rosario DJ, Reilly GC, Ali Salah E, Glover M, Bullock AJ, Macneil S. Decellularization and sterilization of porcine urinary bladder matrix for tissue engineering in the lower urinary tract. Regen Med, 2008, 3(2):145-56.
17. Parekh A, Mantle B, Banks J, Swarts JD, Badylak SF, Dohar JE, Hebda PA. Repair of the tympanic membrane with urinary bladder matrix. Laryngoscope, 2009, 119(6):1206-1213.
18. Nieponice A, McGrath K, Qureshi I, Beckman EJ, Luketich JD, Gilbert TW, Badylak SF. An extracellular matrix scaffold for esophageal stricture prevention after circumferential EMR. Gastrointest Endosc, 2009, 69(2):289-296.
19. Gilbert T W, Gilbert S, Madden M, Reynolds SD, Badylak SF. Morphologic assessment of extracellular matrix scaffolds for patch tracheoplasty in a canine model. Ann Thorac Surg, 2008, 86(3):967-974.
20. Huber JE, Spievack A, Simmons-Byrd A, Ringel R L, Badylak S. Extracellular matrix as a scaffold for laryngeal recon-struction. Ann Otol Rhinol Laryngol, 2003, 112(5):428-433.
21. Jiang WC, Cheng YH, Yen MH, Chang Y, Yang VW, Lee OK. Cryo-chemical decellularization of the whole liver for mesenchymal stem cells-based functional hepatic tissue engineering. Biomaterials, 2014, 35(11):3607-3617.
22. Uygun BE, Soto-Gutierrez A, Yagi H, Izamis ML, Guzzardi MA, Shulman C, Milwid J, Kobayashi N, Tilles A, Berthiaume F, Hertl M, Nahmias Y, Yarmush ML, Uygun K. Organ reengineering through development of a trans-plantable recellularized liver graft using decellularized liver matrix. Nat Med, 2010, 16(7):814-820.
23. Ott HC, Matthiesen TS, Goh SK, Black LD, Kren SM, Netoff TI, Taylor DA. Perfusion-decellularized matrix: using nature's platform to engineer a bioartificial heart. Nat Med, 2008, 14(2):213-221.

24. Lu TY, Lin B, Kim J, Sullivan M, Tobita K, Salama G, Yang L. Repopulation of decellularized mouse heart with human induced pluripotent stem cell-derived cardiovascular progenitor cells. Nat Commun, 2013, 4:2307.

25. Guan Y, Liu S, Liu Y, Sun C, Cheng G, Luan Y, Li K, Wang J, Xie X, Zhao S. Porcine kidneys as a source of ECM scaffold for kidney regeneration. Mater Sci Eng C Mater Biol Appl, 2015, 56:451-456.

26. Goh SK, Bertera S, Olsen P, Candiello JE, Halfter W, Uechi G, Balasubramani M, Johnson SA, Sicari BM, Kollar E, Badylak SF, Banerjee I. Perfusion-decellularized pancreas as a natural 3D scaffold for pancreatic tissue and whole organ engineering. Biomaterials, 2013, 34(28):6760-6772.

27. Moffat D, Ye K, Jin S. Decellularization for the retention of tissue niches. J Tissue Eng, 2022, 13:20417314221101151.

28. Simsa R, Padma AM, Heher P, Hellström M, Teuschl A, Jenndahl L, Berghm N, Fogelstrand P. Systematic in vitro comparison of decellularization protocols for blood vessels. PLoS One, 2018, 13(12):e0209269.

29. Xu H, Xu B, Yang Q, Li X, Ma X, Xia Q, Zhang Y, Zhang C, Wu Y, Zhang Y. Comparison of decellularization pro-tocols for preparing a decellularized porcine annulus fibrosus scaffold. PLoS One, 2014, 9(1):e86723.

30. Xing Q, Yates K, Tahtinen M, Shearier E, Qian Z, Zhao F. Decellularization of fibroblast cell sheets for natural extra-cellular matrix scaffold preparation. Tissue Eng Part C Methods, 2015, 21(1):77-87.

31. Fernández-Pérez J, Ahearne M. The impact of decellularization methods on extracellular matrix derived hydrogels. Sci Rep, 2019, 9(1):14933.

32. McCrary MW, Vaughn NE, Hlavac N, Song YH, Wachs RA, Schmidt CE. Novel Sodium Deoxycholate-Based Chemical De-cellularization Method for Peripheral Nerve. Tissue Eng Part C Methods, 2020, 26(1):23-36.

33. Hwang J, San BH, Turner NJ, White LJ, Faulk DM, Badylak SF, Li Y, Yu SM. Molecular assessment of collagen denaturation in decellularized tissues using a collagen hybridizing peptide. Acta Biomater, 2017, 5:268-278.

34. Lusimbo WS, Leighton FA, Wobeser GA. Histology and ultrastructure of the chorioallantoic membrane of the mallard duck (Anas platyrhynchos). Anat Rec, 2000, 259(1):25-34.

35. Nowak-Sliwinska P, Segura T, Iruela-Arispe ML. The chicken chorioallantoic membrane model in biology medicine and bioengineering. Angiogenesis, 2014, 17(4):779-804.

36. Mîndrilă I, Buteică SA, Mihaiescu DE, Burada F, Mîndrilă B, Predoi MC, Pirici I, Fudulu A, Croitoru O. Magnetic nanoparticles-based therapy for malignant mesothelioma. Rom J Morphol Embryol, 2017, 58(2):457-463.

37. Chu PY, Koh AP, Antony J, Huang RY. Applications of the Chick Chorioallantoic Membrane as an Alternative Model for Cancer Studies. Cells Tissues Organs, 2022, 211(2):222-237.

38. Buteică SA, Mihăiescu DE, Rogoveanu I, Mărgăritescu DN, Mîndrilă I. Chick chorioallantoic membrane model as a preclinical tool for nanoparticles biology study. Rom. Biotechnol. Lett, 2016, 21:11688-11694.

39. Oliinyk D, Eigenberger A, Felthaus O, Haerteis S, Prantl L. Chorioallantoic Membrane Assay at the Cross-Roads of Adipose-Tissue-Derived Stem Cell Research. Cells, 2023, 12(4):592.

40. Dew L, English WR, Chong CK, MacNeil S. Investigating Neovascularization in Rat Decellularized Intestine: An In Vitro Platform for Studying Angiogenesis. Tissue Eng Part A, 2016, 22(23-24):1317-1326.

41. Moreno-Jiménez I, Hulsart-Billstrom G, Lanham SA, Janeczek AA, Kontouli N, Evans ND, Oreffo ROC. The chorioallantoic membrane (CAM) assay for the study of human bone regeneration: a refinement animal model for tissue engineering. Sci Rep, 2016, 6:32168.

42. McInnes AD, Moser MAJ, Chen X. Preparation and Use of Decellularized Extracellular Matrix for Tissue Engineering. J Funct Biomater, 2022, 13(4):240.

43. Hussey GS, Dziki JL, Badylak SF. Extracellular matrix-based materials for regenerative medicine. Nat. Rev. Mater, 2018, 3:159-173.

44. Kawecki M, Łabuś W, Klama-Baryla A, Kitala D, Kraut M, Glik J, Misiuga M, Nowak M, Bielecki T, Kasperczyk A. A review of decellurization methods caused by an urgent need for quality control of cell-free extracellular matrix' scaffolds and their role in regenerative medicine. J Biomed Mater Res B Appl Biomater, 2018, 106(2):909-923.

45. Tenreiro MF, Louro AF, Alves PM, Serra M. Next generation of heart regenerative therapies: progress and promise of car-diac tissue engineering. Regen Med, 2021, 6:30.

46. Kc P, Hong Y, Zhang G. Cardiac tissue-derived extracellular matrix scaffolds for myocardial repair: advantages and chal-lenges. Regen Biomater, 2019, 6(4):185-199.

47. Chakraborty J, Roy S, Ghosh S. Regulation of decellularized matrix mediated immune response. Biomater Sci, 2020, 8(5):1194-1215.

48. Friedrich EE, Lanier ST, Niknam-Bienia S, Arenas GA, Rajendran D, Wertheim JA, Galiano RD. Residual sodium dodecyl sulfate in decellularized muscle matrices leads to fibroblast activation in vitro and foreign body response *in vivo*. J Tissue Eng Regen Med, 2018, 12(3):e1704-e1715.

49. Sokol AA, Grekov DA, Yemets GI, Galkin AYu, Shchotkina NV, Dovghaliuk AA, Telehuzova OV, Rudenko NM, Romaniuk OM, Yemets IM. Comparison of bovine pericardium decellularization protocols for production of biomaterial for cardiac surgery. Biopolym Cell, 2020, 36:392-403.

50. Aamodt JM, Grainger DW. Extracellular matrix-based biomaterial scaffolds and the host response. Biomaterials, 2016, 86:68-82.

51. Predoi MC, Mîndrilă I, Buteică SA, Purcaru ȘO, Mihaiescu DE, Mărginean OM. Iron Oxide/Salicylic Acid Nanopar-ticles as Potential Therapy for B16F10 Melanoma Transplanted on the Chick Chorioallantoic Membrane. Processes, 2020, 8:706.

Corresponding Author: Ion Mîndrilă, Department of Anatomy, Faculty of Medicine, University of Medicine and Pharmacy of Craiova, e-mail: ion.mindrila@umfcv.ro